



From CORALIE to HARPS The Way Towards 1 m s^{-1} Precision Doppler Measurements

D. QUELOZ¹, M. MAYOR¹

With the collaboration of the CORALIE Team: S. UDRY¹, M. BURNET¹, F. CARRIER¹, A. EGGENBERGER¹, D. NAEF¹, N. SANTOS¹

And for the HARPS Project: F. PEPE¹, G. RUPPRECHT³, G. AVILA³, S. BAEZA², W. BENZ⁵, J.-L. BERTAUX⁶, F. BOUCHY¹, C. CAVADORE³, B. DELABRE³, W. ECKERT², J. FISCHER⁵, M. FLEURY¹, A. GILLIOTTE², D. GOYAK², J.C. GUZMAN², D. KOHLER⁴, D. LACROIX⁴, J.-L. LIZON³, D. MEGEVAND¹, J.-P. SIVAN⁴, D. SOSNOWSKA¹, U. WEILENMANN²

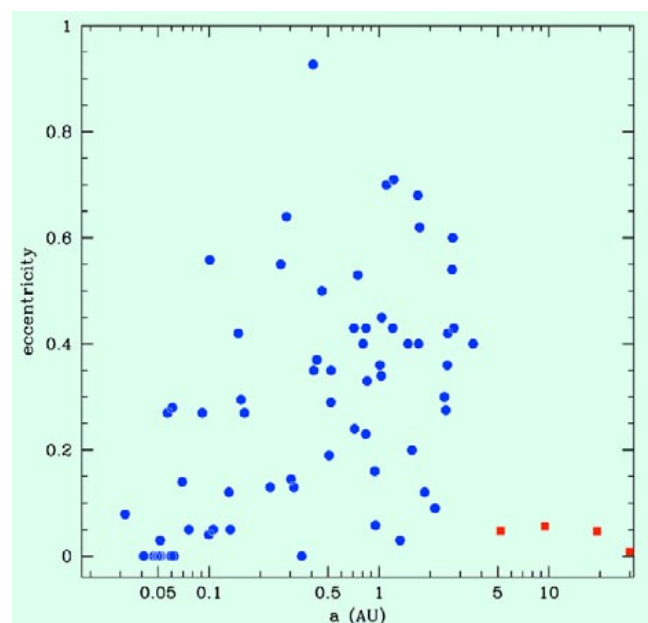
¹Observatoire de Genève; ²ESO, La Silla; ³ESO, Garching; ⁴Observatoire de Haute-Provence; ⁵Physikalisches Institut, Bern; ⁶Service d'Aéronomie

1. Search for Extrasolar Planets by Precise Doppler Measurements

Precise Doppler measurements of stars is a very efficient way to search for extrasolar planets orbiting nearby stars similar to the Sun. The gravitational interactions between a planet and its host star produces a change of the radial velocity of the star that can be detected by Doppler measurements with precision of few m s^{-1} . Thanks to the effort of observations done by precise Doppler surveys conducted world-wide, 67 companions with mass less than $15 M_J$ have been discovered. Today ongoing surveys regularly monitor the radial velocity of a total sample of 3000 G, K and M stars (Queloz 2001).

The detection of a planet by the measurement of the orbit of its host star brings information on the mass of the planet, the orbital eccentricity and the orbital period. Actually the mass is only known within the uncertainty of the projection factor represented by the $\sin i$ of the orbit. However, the $\sin i$ statistics is so sharp that one has 87% probability to be within a factor of 2 ($\sin i$ between 1 and 0.5).

Figure 1: Semi-major axis and eccentricity distribution of the extra-solar planets (blue dots) discovered as of July 2001. In red squares are shown the giant planets of the Solar System.



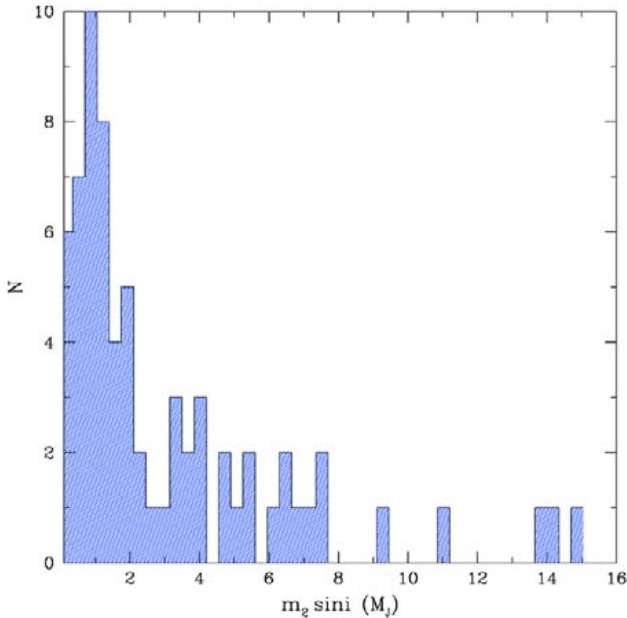


Figure 2: Extra-solar planet mass distribution. Below $1 M_J$ the mass distribution is biased by the detection threshold that makes planets on far-off orbits harder to detect.

The first planet discovered orbiting the star 51 Peg (Mayor & Queloz 1995) is a giant planet on a very close orbit (4.2 days). Other similar systems have been later detected. The direct observation of a transit of one of these short orbit planets (Charbonneau et al. 2000, Mazeh et al. 2000) brought the final confirmation of their existence. These planetary systems, called “hot Jupiters”, do not fit in the paradigm of the planet formation based on the observation of our Solar System (Boss 1995; Lissauer 1995). Extra mechanisms such that planet migration or multi-planet gravitational interactions have been suggested to explain their formation (see references in the review by Marcy et al. 2000).

The orbital characteristics of the extrasolar planets detected so far contrast with the orbital characteristics of giant planets in our solar system (see Fig. 1). The orbits of giant planets in our Solar System are almost circular, a natural consequence of their formation in the protoplanetary disk. The extrasolar planets show a wide range of eccentricity surprisingly similar to the eccentricity distribution of binary systems with stellar companions (Mayor & Udry 2000). This is not understood in the frame of a global planetary formation theory. However the interpretation of data should be made carefully and specifically the comparison with our solar system. Actually ongoing planet surveys have not been able yet to detect a Jupiter analogue ($1 M_J$ object at or above 5 AU). The orbit of Jupiter produces on the Sun a complete radial velocity variation of 13 m s^{-1} amplitude in 11 years. Intensive high-precision Doppler surveys while reaching enough precision (about 3 m s^{-1}) do not yet

have enough time coverage. Extra years of measurements are needed to tackle Jupiter mass planets with orbital periods longer than 10 years. Moreover, it is important to recall that Doppler surveys are sensitive to a detection systematic that ties together the mass of the planet with the semi-major axis of its orbit, making easier the detection of a planet on a short orbit than of a planet like Jupiter.

Doppler surveys are providing the first results on planet mass distribution. While we can still debate on the maximum mass of planets (See Jorissen et al. 2001) we know for sure that the planet mass function is dramatically rising towards low masses (Fig. 2). If we restrict the analysis to planets with masses larger than $1 M_J$ and with orbits having semi-major axes less than 3 AU we find a rise $dn/dm \sim m^{-1}$. Below $1 M_J$ the detection threshold limits the detection to systems on shorter orbits, therefore the observed mass function artificially decreases. With the reasonable assumption that the planet mass function should continue to rise at least in the giant planet mass domain, we can expect that any improvements in the detection threshold should convert into a significant increase of the planet detection rate.

The studies of the content of the atmosphere of stars having a planet show spectroscopic features that distinguish them from field stars with no planet detection. Statistically the stars with planets are metal richer compared to stars with no planet detection (Santos et al. 2001). A recent study on the Li^6 content of the atmosphere of the star HD 82943, hosting a planet, suggests that extra Lithium has been brought to the atmosphere of that star, possibly fed by a planet (Israelian et al. 2001). These observations rise the issue of a possible trace of the planet

Figure 4: Perspective drawing of CORALIE. The fibre entrance is on the left. The grating is coloured in green.

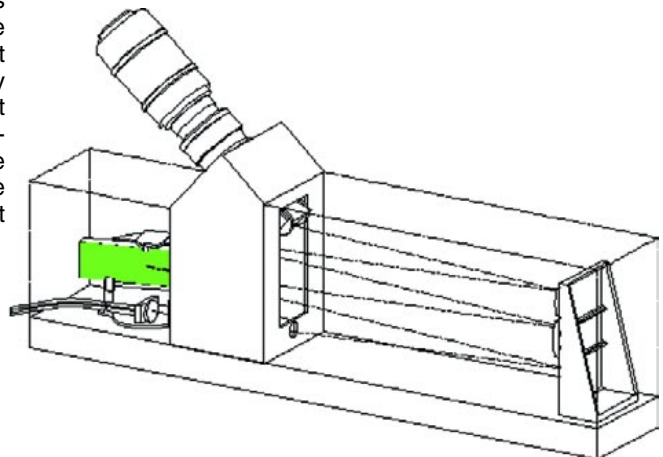


Figure 3: 1.2-m Swiss Leonard Euler telescope at La Silla. The CORALIE front-end adapter is visible at the Nasmyth focus on the top of the right fork of the telescope.

formation visible in the atmosphere of the star.

2. The CORALIE Spectrograph

CORALIE is the fibre-fed echelle spectrograph installed in April 1998 at the Swiss 1.2-m Leonard Euler telescope at the ESO La Silla Observatory (Fig. 3). It has been built as a joint project with the Observatoire de Haute-Provence which owns the first specimen, named ELODIE (Baranne et al. 1997; Queloz et al. 2000). The CORALIE spectrograph is fed by two fibres each including a double scrambler device to improve the stability of the input illumination of the spectrograph. The spectrograph itself is located in an isolated and stable environment with an accurate temperature regulation. The fibres are connected to the Euler telescope Nasmyth focus by a front-end adapter. The calibration lamps and the entrance fibre viewer device are part of the front-end adapter.

The optical design of CORALIE is the same as that of ELODIE. The echelle grating is used with $\tan \phi = 4$ blaze angle and the cross-disperser is made of a prism and a grism in order to obtain equal spacing between orders through the whole useful wavelength range. The optical system is made of numerous surfaces but allows a compact image with a maximal resolution of 100,000. (See Fig. 4 and Table 2.)

CORALIE has been designed to achieve precise radial velocity measurements and to deliver the measurements shortly after the end of the exposure. The telescope and the spectrograph are operated by a single observer in a semiautomatic mode. The sequence of observations can be prepared before the beginning of the night and run automatically during the night.

The measurements of stellar radial velocities at a few meter per second precision rely on two key elements. First, one needs enough photons and spectral information to compute the radial velocity with a high precision. Second, one needs a stable reference to measure and to correct the systematic errors of the instrument. The 3000 Å wavelength range ensures a rich spectral information for the computation of the radial velocity balancing the modest size of the telescope. For example, for a K0 dwarf with $v \sin i = 2 \text{ km s}^{-1}$ we reach in 10 minutes a 3 m s^{-1} precision on the radial velocity measurement for a 7.5 magnitude star. The stable reference is provided by the intrinsic very high stability of the instrument itself and regular wavelength calibrations with the thorium spectrum. Moreover, the simultaneous use of the thorium during science exposures corrects from any short-term drifts of the instrument. The technique is known as the simultaneous thorium referencing technique (Queloz et al. 1999). On Figure 5 a CORALIE CCD frame with a simultaneous thorium reference is displayed.

CORALIE has an automatic reduction software that provides fully calibrated spectra and a measurement of the radial velocity by cross-correlation. The general description of this software can be found in (Baranne et al. 1996). Since the CORALIE commissioning, significant modifications in reduction algorithms have been made, leading to an improvement of the long-term precision from 7 m s^{-1} to 2 m s^{-1} (rms).

The long-term reference is provided by the thorium spectrum. The procedure setting the global wavelength solution has been modified in 2001. The wavelength solution fit includes a weighting scheme that takes into account positioning uncertainties of the photo centre of each pixel (about 50 m s^{-1}). The fit of the global wavelength solution is done with 1200 thorium spectral lines. The fit on the solution has 80



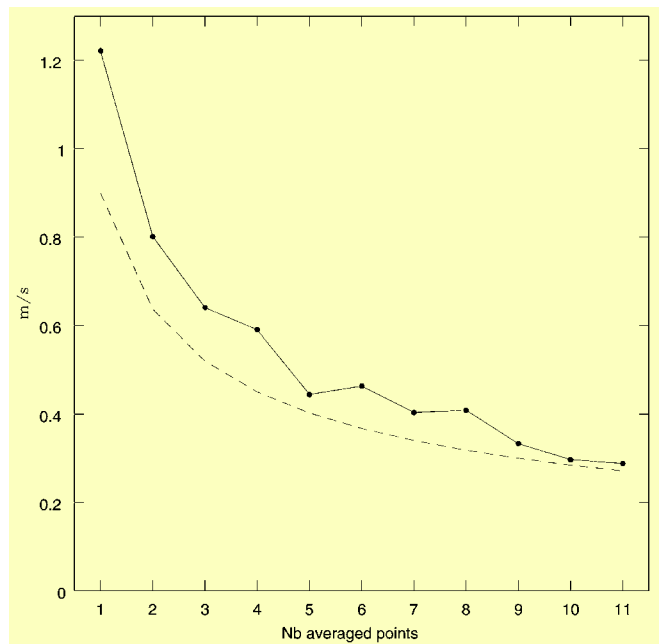
Figure 5: CCD frame of a CORALIE stellar exposure with its simultaneous thorium reference. The emission lines (black dots) of the thorium spectrum are clearly visible between the orders of the stellar spectrum

m s^{-1} rms residual, corresponding to 2 m s^{-1} error on the zero point of the calibration.

The short-term tracking of the instrument by simultaneous thorium shows no instrument error apart the photon noise (Fig. 6). The measured dispersion of a sequence of radial velocity measurements on the Sun is 1.2 m s^{-1} . Part of it comes from the solar oscilla-

tion signal, the rest from the photon noise on the measurement of the instantaneous drift of the instrument. When we average the measurements, the sun oscillation signal averages as well. The convergence of the observed dispersion with the expected dispersion due to the photon noise demonstrates that no extra instrumental noise is seen down to 30 cm s^{-1} . This result

Figure 6: Observed radial velocity dispersion on a 4-hour observation sequence of the Sun. We display the dispersion for different numbers of averaged measurements in order to average the Sun oscillation signal as well. The hatched curve indicates the expected uncertainties on the radial velocity from the photon-noise error on the measurement of the simultaneous tracking. With an average of 10 radial-velocity measurements we average out the solar oscillation signal.



Planet name	$m_2 \sin i$ M_J	a [AU]	O–C $m s^{-1}$	Discovery
Gl86b	3.4	0.11	9	1998
HD192263b	0.68	0.15	11	1999
HD130322b	0.95	0.32	15	1999
HD83443c	0.15	0.17	6	2000
HD168746b	0.23	0.07	9	2000
HD108147b	0.31	0.10	11	2000
HD83443b	0.34	0.04	6	2000
HD75289b	0.40	0.04	8	2000
HD6434b	0.44	0.15	14	2000
HD121504b	0.81	0.32	9	2000
HD52265b	0.98	0.50	11	2000
HD19994b	1.7	1.23	10	2000
HD169830b	2.8	0.82	10	2000
HD1237b	3.2	0.49	11	2000
HD92788b	3.4	0.97	12	2000
HD162020b	13	0.07	13	2000
HD202206b	13.6	0.76	11	2000
HD168443c	13.7	2.67	6	2000
HD82943c	0.80	0.73	7	2001
HD82943b	1.48	1.16	7	2001
HD213240b	3.3	1.6	12	2001
HD28185b	5.3	1.01	10	2001
HD141937b	8.8	1.49	11	2001

Table 1: List of Extra-solar planets discovered by CORALIE. In the O–C column are the residuals to the planet model fit. Residuals higher than $10 m s^{-1}$ usually origin from stellar intrinsic activity at the surface of some young star or they suggest another companion yet undetected. References can be found on <http://obswww.unige.ch/~udry/planet/planet.html>

makes possible asteroseismology programmes to detect Solar-type oscillations by radial velocity measurements on dwarf stars.

The long-term precision of radial velocity measurements is tied to the quality and the reliability of the daily zero points. Actually no systematics have been observed apart the $2 m s^{-1}$ error on the wavelength calibration. The bright star 82 Eri is one of the star used since the installation of CORALIE as a proxy for the long-term precision tracking. We measure a $3.6 m s^{-1}$ dispersion over a 2.5-year duration with no indications of long-term systematics (Fig. 7). Moreover, the yearly average has a dispersion less than $1 m s^{-1}$. It demonstrates that in few years, with a longer time-base, the detection of Jupiter-mass objects on far-off orbits similar to our giant planets Jupiter or even Saturn is to be expected.

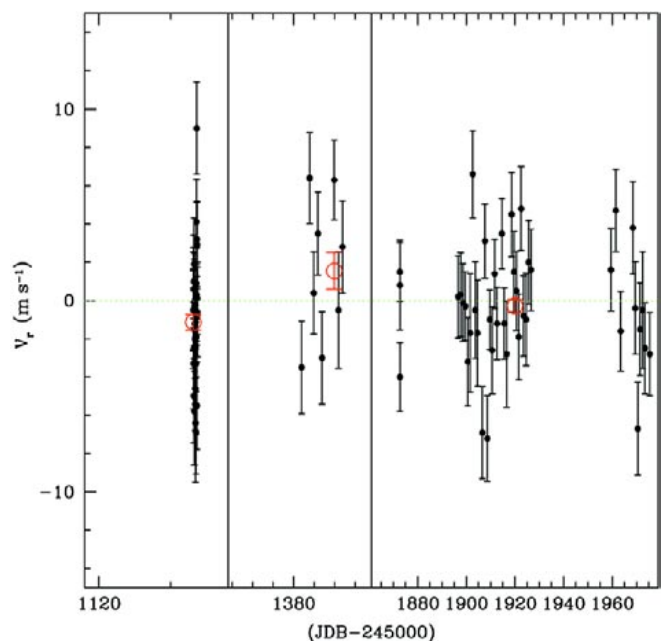
3. The CORALIE Planet Search Programme

In mid-1998, right after the successful commissioning of CORALIE, started the CORALIE planet search programme. The survey sample is made of 1650 dwarf stars, brighter than 10th V-mag located in the southern hemisphere, selected according to their distance from the Sun. Actually, different distance criteria have been used for G and K dwarfs in order to compensate for the magnitude difference between spectral types (see in Udry et al. 2000). In the sample 80% of the stars are brighter than 9th V-mag. Active stars

and fast rotators are not excluded from the sample but once they are identified they are observed with a lower priority. The exposure time of each observation is set to reach a photon-noise error of about $5 m s^{-1}$ per radial-velocity measurement. It corresponds to a signal-to-noise ratio per pixel between 30 and 100, depending on the spectral type.

After three years of activity the planet search programme totals 14,000 precise radial velocity measurements. CORALIE has discovered 23 extrasolar planets (Table 1) and contributed to the precise measurement of orbital characteristics of 5 other planets. Amongst the many discoveries made by CORALIE, a very interesting multiple system is displayed in Figure 8. This multiple sys-

Figure 7: Radial velocity measurements of the bright G8 star 82 Eri. The dispersion of the data is $3.6 m s^{-1}$. In red we indicate the yearly average. The dispersion of the yearly average is less than $1 m s^{-1}$, suggesting no instrumental systematics down to this level.



tem is made of two Saturn-mass objects trapped in a 1:10 resonance.

4. Catching the Sound of Stars with CORALIE

Acoustic waves or solar oscillations are observed on the Sun. They are thought to be excited by turbulent convection near the surface. Observations of solar oscillations place important constraints on the internal structure of the Sun and provides a strong test of evolutionary theory as well. The radial velocity effect from the 5-min solar oscillations has a radial velocity amplitude of $23 cm s^{-1}$. Many attempts have been made, to detect similar oscillations on other stars. With CORALIE we have been able to detect for the first time an unambiguous oscillation signal of $31 cm s^{-1}$ amplitude on the star α Centauri A, a nearby solar twin. This corresponds to a wave with an amplitude of 40 metres at the surface of that star.

The star α Centauri A was observed with CORALIE during 13 nights in May 2001. In total, 1850 spectra were collected with typical signal-to-noise ratios in the range 300–420 at 550 nm. The radial-velocity measurement sequence shows a dispersion of $1.53 m s^{-1}$. The power spectrum shown in Figure 9 exhibits a series of peaks between 1.8 and 2.9 mHz modulated by a broad envelope. This is the typical signature of solar-like oscillations (Bouchy & Carrier 2001).

In the low frequency range of the power spectrum ($\nu < 0.6 mHz$), the power of the signal scales inversely to the square of the frequency as expected for a white noise contribution. The mean white noise level in the power spectrum, computed in the range 0.6–1.5 mHz, is $4.3 cm s^{-1}$ corresponding to a velocity precision of $1.0 m s^{-1}$ per measurement.

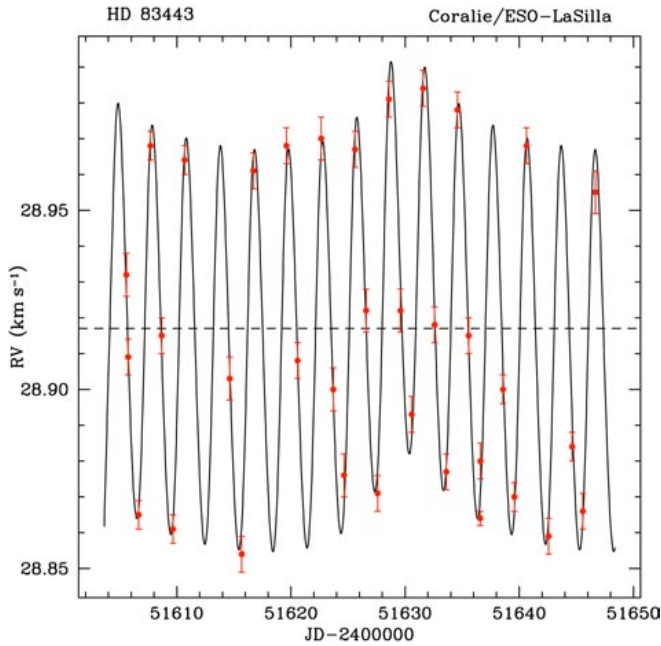


Figure 8: Radial-velocity measurements of the star HD 83443. The curve is the best fit to the data with a two-planet model. The period of the shortest orbit is 2.9853 d and the long one is 29.85 d. Both planets have about the same mass as Saturn. Interestingly, the system may be trapped in a 1:10 resonance.

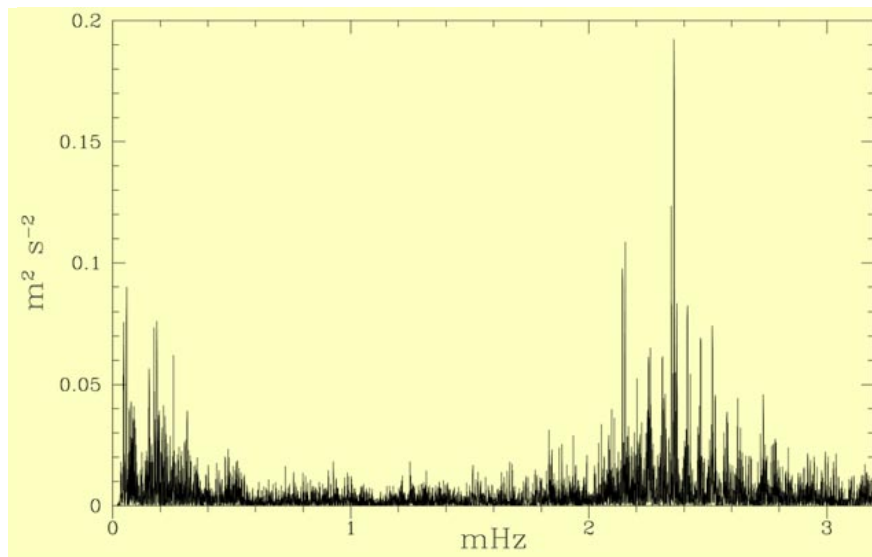
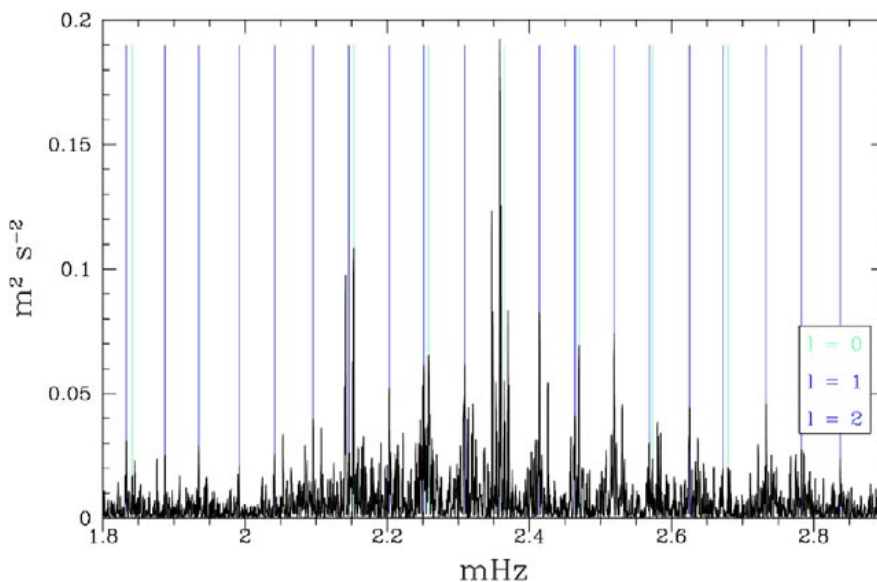


Figure 9: Power spectrum of 13 nights of radial-velocity measurements on the star α Cen A. The series of peaks between 1.8 and 2.9 mHz is the signature of solar-like oscillations.



The strongest modes are identified in Figure 10. From the measurement of the large splitting ($\Delta\nu = \nu_{n,l} - \nu_{n-1,l}$) and the small splitting ($\delta\nu_0 = \nu_{n,0} - \nu_{n-1,2}$) we constrain the mass and the age of the star. Preliminary results (Carrier et al. 2001) suggest that α Cen A is slightly more evolved than the Sun, with a mass in the range 1.10–1.16 M_{\odot} .

5. HARPS: the 1 m s⁻¹ Precision Instrument

HARPS is a fibre-fed, cross-dispersed echelle spectrograph design to measure radial velocities of stars with a precision better than 1 m s⁻¹. It will be installed on the 3.6-m ESO telescope at La Silla, Chile. HARPS is the result of an Announcement of Opportunity made by ESO in 1998 for the design, the construction, and procurement of a High-Accuracy Radial velocity Planetary Searcher (HARPS) instrument.

In response to ESO's announcement the Observatoire de Genève has formed a Consortium that has been reinforced considerably by the active participation of the ESO La Silla Observatory and the ESO Garching Cryogenic Group and Optical Detector Team. At present, all design reviews have been passed and the project is in its manufacturing phase. The instrument commissioning is scheduled for the end of 2002. Besides the guarantee time for the Consortium, a large amount of HARPS time will be available to the astronomical community for a broad variety of observational programmes in different domains including for example the search for extrasolar planets and asteroseismology.

The strategic choices of the HARPS project are based on the experience gathered with the ELODIE and the CORALIE instruments. Moreover, to cope with the short track development of the project we have tried to avoid as much as possible any development risk that could jeopardise the project. In general, we preferred to adopt conservative solutions every time the consequences of a proposed new solution on the final result were not known precisely. HARPS design is based on three fundamental technical choices. First, we decided to adopt a fibre-fed illumination with two fibres for simultaneous thorium referencing. Apart the fact that this technique has already proven its efficiency with ELODIE and CORALIE, it is about 4–6 times

Figure 10: Identified p-mode oscillations in the power spectrum of radial-velocity measurements of α Cen A. l corresponds to the number of knots of the various pulsation orders (n -number), where $l = 0$ is the radial pulsation. Typical identified pulsation mode n -numbers range from 15 to 25.

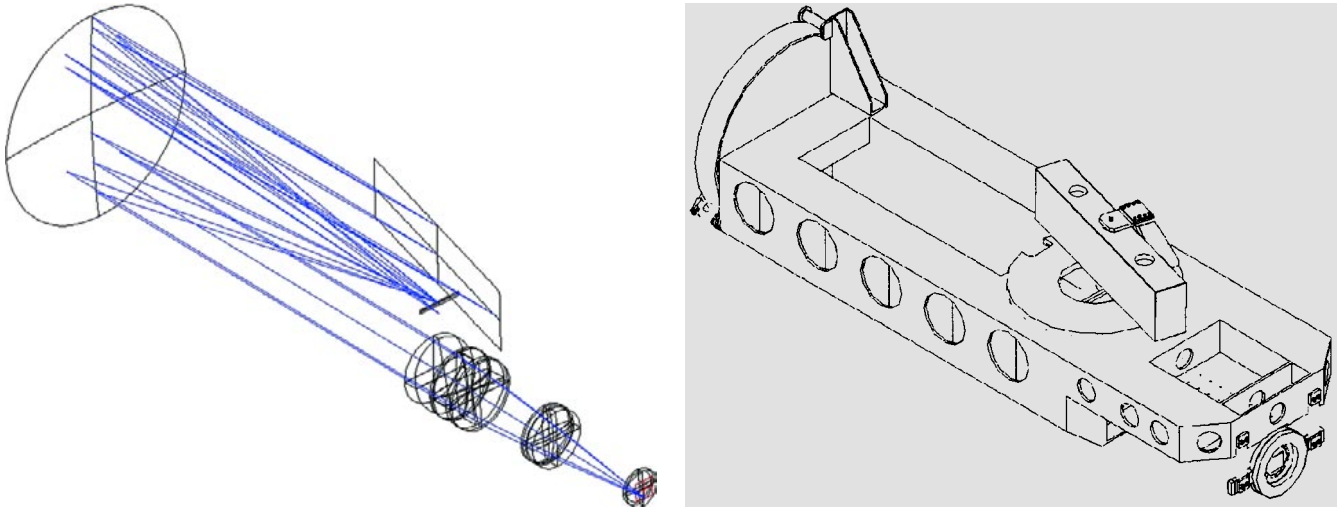


Figure 11: Ray tracing of the HARPS optical design. The optical design is very similar to that of UVES. The main difference is the use of a grism for the cross disperser instead of a reflection grating. This solution is more stable and allows a compact mechanical mount.

more efficient in terms of photon need than using an alternative technique like the iodine cell for example (Bouchy et al. 2001). A fundamental aspect to reach 1 m s^{-1} accuracy on a large sam-

ple of stars. Second, we decided to build an instrument using the largest monolithic echelle grating available ($837 \times 208 \text{ mm}$ grating developed for UVES) in order to achieve a very high spectral resolution. For stars with unresolved absorption lines, the precision of the measurement of the radial velocity scales with the 1.5 power of the spectral resolution (Hatzes & Cochran

1992). A good compromise between slit losses and best resolution was finally found to be $R = 90,000$. More complex solutions for increasing the efficiency and the spectral resolution, like for example using adaptive optics or an image slicer, have been considered but were found not suitable for HARPS. Finally, while the simultaneous thorium referencing technique monitors the instrumental drifts in order to remove them, we made additional efforts to increase the intrinsic opto-mechanical stability of the spectrograph. In order to eliminate the atmospheric pressure variation, which could produce wavelength drifts ($100 \text{ m s}^{-1}/\text{mbar}$) and to exclude any convective cell circulation in the spectrograph, the entire spectrograph is operated in vacuum. Moreover, the vacuum vessel protects the spectrograph from rapid temperature variations. The vacuum vessel itself is installed inside a temperature-controlled environment which ensures a long-term stability better than 0.1 K . To improve the stability of the spectrograph input illumination as well, each fibre includes a double scrambler. More details on HARPS design can be found in Pepe et al. 2000.

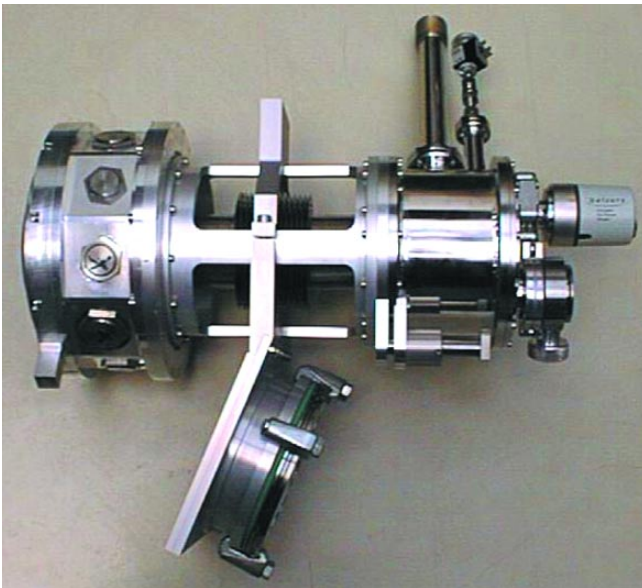


Figure 12: The HARPS dewar consisting of the detector head, the cryostat, and the interface below. The rigid central part replaces the vacuum vessel and allows to simulate the working condition of the dewar.

Table 2: Spectrograph characteristics.

	HARPS	CORALIE
Optical design	fibre-fed, cross-dispersed echelle spectrograph	
# of fibres	2 (object and reference)	
Accepted field on sky	1 arcsec	2 arcsec
Collimated beam diameter	208 mm	100 mm
Covered spectral range	380 nm to 690 nm	
Spectral format	68 echelle orders	
	$61.44 \times 62.74 \text{ mm}$	$26 \times 26 \text{ mm}$
Spectral resolution	90,000	50,000
CCD chip	mosaic, $2 \times \text{EEV } 2\text{k}4$	EEV $2\text{k}2$
	pixel size = $15 \mu\text{m}$	pixel size = $15 \mu\text{m}$
Sampling/Spectral element (FWHM)	4 pixels	3.3 pixels
Image quality	< 1.5 pixels	< 1.5 pixels
Minimum inter-order spacing	30 pixels	10 pixels
Spectrograph peak efficiency at 550 nm	28 %	7%
Total peak efficiency at 550 nm	4.5%	1.5%

The optical design, proposed by B. Delabre and adapted by D. Kohler, is very similar to that of UVES. A ray tracing of the optical design is shown in Figure 11. Two fibres, an object and a reference fibre feed the spectrograph with the light from the telescope. The fibres are re-imaged by the spectrograph optics onto a mosaic of two $2 \times 4 \text{ k}$ CCDs (EEV, $15 \mu\text{m}$), where two echelle spectra of 68 orders are formed. The spectral domain ranges from 380 nm to 690 nm with no order lost for the object fibre. A summary of the spectrograph's parameters is given in Table 2.

Realisation of the spectrograph's opto-mechanics is under the responsibility of the Observatoire de

Figure 13: The Cassegrain Fibre Adapter body during manufacturing at La Silla, ESO.



Haute-Provence and made in collaboration with the Physikalisches Institut of the Bern University. The spectrograph optics is mounted on a 2.5-metre optical bench made of plated steel. The orientation of the optical plane is vertical, the echelle grating being mounted on the top side, and the grism and the camera on the bottom side of the bench (Figure 11).

HARPS uses a standard VLT detector head and the ESO controller FIERA. ESO's Optical Detector Team will provide the Consortium with the Detector Unit including detector-head electronics, the LCU, and the Continuous-Flow Cryostat adapted by the ESO Cryogenic group to the HARPS-specific vacuum vessel solution (See Fig. 12).

The vacuum vessel containing the spectrograph will be installed inside the air-conditioned coudé room. It is manufactured under the responsibility of the Geneva Observatory. It consists of a polished stainless steel vessel of 1 m diameter and about 3 m long, evacuated at about $p = 10^{-2}$ mbar.

The HARPS Cassegrain Fibre Adapter is the interface to the telescope. It is entirely made by the La Silla Observatory. It incorporates several instrumental functions and an Atmospheric Dispersion Corrector (ADC). It is presently in an advanced realisation phase (see Fig.13).

HARPS should be an unrivalled facility for conducting planet search programmes and asteroseismology measurements. The improvement made on HARPS compared to CORALIE will reduce the instrumental errors well below the 1 m s^{-1} threshold. The expected performances of HARPS are shown in Figure 14. For a G8 dwarf star a radial-velocity measurement at 1 m s^{-1} accuracy is reached in 1 minute exposure for a star of magnitude 7.5. More details on the photon-noise errors of radial-velocity measurements for different stellar spectral types and different $v \sin i$ can be found in Bouchy et al. (2001).

References

- Baranne, A., Queloz D., Mayor M. 1996, et al., *AASS* **119**, 373.
 Boss, A., 1995, *Science* **267**, 360.
 Bouchy, F., Carrier, F., 2001, *A&A*, **374**, L5.
 Bouchy, F., Pepe, F., Queloz, D., 2001, *AA* **374**, 733.
 Butler, R.P., Marcy, G.W., Williams, E., et al. 1996, *PASP* **108**, 500.

- Carrier, F., Bouchy, F., Provost, J., et al., 2001, *IAU Colloquium* **185**, in press.
 Charbonneau D., Brown, T., Latham, D., Mayor, M., *ApJ* **529**, L45.
 Hatzes, A.P., Cochran, W.D., 1992, in "Workshop on High-Resolution Spectroscopy with the VLT", M. Ulrich, ed., 275.
 Israelian, G., Santos, N. C., Mayor, M., Rebolo, R. 2001, *Nature* **411**, 163.
 Jorissen, A., Mayor, M., Udry, S., 2001, *A&A* submitted, astro-ph/0105301.
 Lissauer, J. 1995, *Icarus* **114**, 217.
 Marcy, G., Cochran, W.D., Mayor, M., 2000, *PPIV*, V. Mannings, A.P. Boss, S.S. Russell ed., 1285.
 Mazeh, T., Naef, D., Torres, G., et al., 2000, *ApJ* **532**, L55.
 Mayor M. Queloz, D. 1995, *Nature* **378**, 355.
 Mayor, M., Udry, S., 2000, in "Disks, planetesimals and Planets", F. Garzon, C. Eiroa, D. de Winter and T.J. Mahoney Eds., ASP Conf. Ser. **219**, 441.
 Pepe, F., Mayor M., Delabre B., et al., 2000, in "Optical and IR Telescope Instrumentation and Detectors" *SPIE* **4008**, 582.
 Queloz, D., Casse, M., Mayor, M., 1999, *ASP Conf Ser.* **185**, 13.
 Queloz D., Mayor M., Naef D., et al., 2000, In "VLT Opening symposium opening: From Extrasolar Planets to Brown dwarfs", J. Bergeron & A. Renzini (eds.), *ESO Astrophysics Symposia Ser.*, **548**.
 Queloz, D., 2001, in "11th Cool stars, stellar systems and the Sun", ASP Conf Ser. **223**, R.J. Garcia Lopez, R. Rebolo, M. R. Zapatero Osorio (eds), 59.
 Santos, N.C., Israelian, G., Mayor, M., 2001, *A&A* **373**, 1019.
 Udry, S., Mayor, M., Naef, D., et al., 2000, *A&A*, **356**, 590.

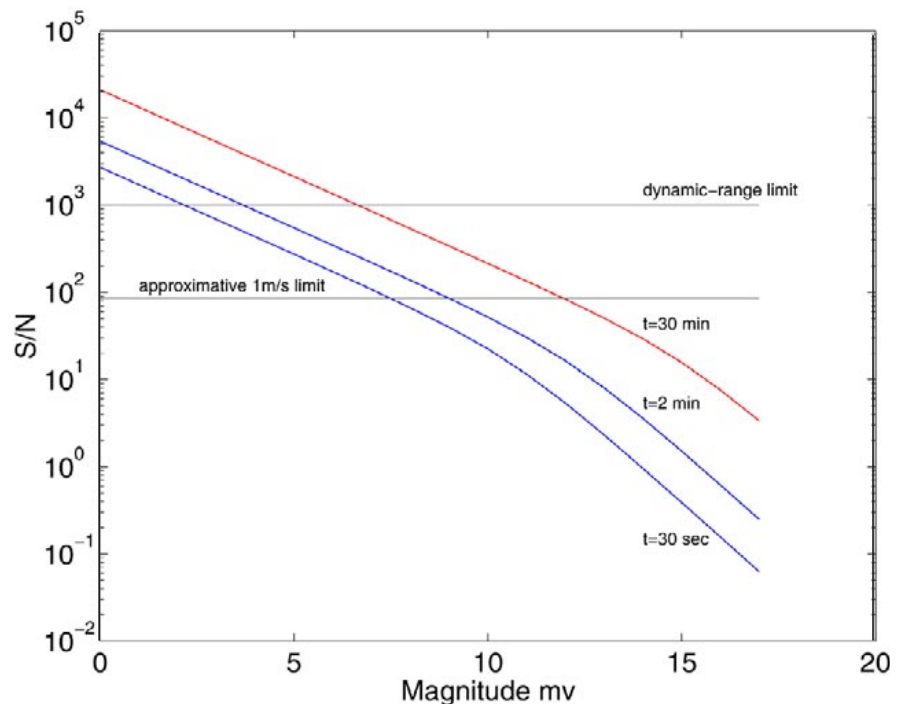


Figure 14: Signal-to-noise ratio per spectral bin at $\lambda = 550 \text{ nm}$. The dynamic range of the CCD and the estimated 1 m s^{-1} limit for a G8 star are shown.